

Article

Automated Quality Inspection of Formwork Systems Using 3D Point Cloud Data

Keyi Wu , Samuel A. Prieto * , Eyob Mengiste  and Borja García de Soto 

S.M.A.R.T. Construction Research Group, Division of Engineering, New York University Abu Dhabi (NYUAD), Experimental Research Building, Saadiyat Island, Abu Dhabi P.O. Box 129188, United Arab Emirates; keyi.wu@nyu.edu (K.W.); eyob.mengiste@nyu.edu (E.M.); garcia.de.soto@nyu.edu (B.G.d.S.)

* Correspondence: samuel.prieto@nyu.edu

Abstract: Ensuring that formwork systems are properly installed is essential for construction safety and quality. They have to comply with specific design requirements and meet strict tolerances regarding the installation of the different members. The current method of quality control during installation mostly relies on manual measuring tools and inspections heavily reliant on the human factor, which could lead to inconsistencies and inaccurate results. This study proposes a way to automate the inspection process and presents a framework within which to measure the spacing of the different members of the formwork system using 3D point cloud data. 3D point cloud data are preprocessed, processed, and analyzed with various techniques, including filtering, downsampling, transforming, fitting, and clustering. The novelty is not only in the integration of the different techniques used but also in the detection and measurement of key members in the formwork system with limited human intervention. The proposed framework was tested on a real construction site. Five cases were investigated to compare the proposed approach to the manual and traditional one. The results indicate that this approach is a promising solution and could potentially be an effective alternative to manual inspections for quality control during the installation of formwork systems.

Keywords: 3D laser scanning; concrete construction; construction automation; data processing and analysis; quality inspection; temporary structure



Citation: Wu, K.; Prieto, S.A.; Mengiste, E.; García de Soto, B. Automated Quality Inspection of Formwork Systems Using 3D Point Cloud Data. *Buildings* **2024**, *14*, 1177. <https://doi.org/10.3390/buildings14041177>

Academic Editor: Hongping Yuan

Received: 23 January 2024

Revised: 13 March 2024

Accepted: 24 March 2024

Published: 21 April 2024



Copyright: © 2024 by the authors. Licensee MDPI, Basel, Switzerland. This article is an open access article distributed under the terms and conditions of the Creative Commons Attribution (CC BY) license (<https://creativecommons.org/licenses/by/4.0/>).

1. Introduction

In a construction project, the formwork system consists of a set of temporary structures used to mold fresh concrete into the desired appearance, shape, dimension, and location [1]. As a critical element in concrete construction, the formwork system can not only easily cause safety risks during concrete placement (in the case of collapse due to improper installation) but can also seriously affect the quality of resulting concrete structures after the placement [2]. The formwork system occupies a significant proportion of the concrete construction investment, and it is reported to usually account for 40% to 60% of the cost of concrete construction [3]. Overall, the formwork system plays an important role in the smooth progress and successful completion of concrete construction [4].

The design considerations of the formwork system that belongs to a temporary structure, such as loads, materials, and methods, are different from those of permanent structures [5]. The formwork system has many uncertainties and requires quality inspections to ensure sufficient strength, stiffness, and stability [6]. The quality inspection of the formwork system mainly consists of a process to examine, measure, and assess whether the characteristics (e.g., number, size, spacing) of the installed formwork system properly comply with specific design requirements [5]. If the formwork system does not satisfy design requirements, it may not be strong enough and thus cause severe damage or deficiencies to concrete structures, even fatalities in the case of collapse; and if the formwork system exceeds design requirements, it may result in unnecessary waste, such as more resources and cost [4]. Therefore, the quality inspection of the formwork system is of great practical

significance in concrete construction [5]. Recent studies have highlighted the need to integrate automated digital technologies and smart formwork systems to promote effective and sustainable practices in concrete construction [7].

The formwork system typically comprises different categories of members, including panels, studs, wales, ties, and braces, which are highlighted in yellow, purple, green, red, and blue, respectively, in Figure 1. To ensure the strength, stiffness, and stability of the formwork system, the spacing of studs, wales, ties, and braces, as one of the main determinants, needs to be specifically designed according to the force determined by the properties of concrete (e.g., density, initial setting time, slump) and the means and methods of construction (e.g., placement approach, speed), as well as the object determined by the features of the members (e.g., material, size, shape) [4,5]. Generally, the traditional spacing measurement of formwork system members is mainly conducted using manual measuring tools (e.g., measuring tape, laser distance meter). This process is time-consuming and labor-demanding. In addition, it can be affected by the inspector's knowledge and skills, making the collection of data subjective and inconsistent [4,8]. With a system reliant on human perception, there is always a possibility of obtaining incorrect data, which, based on the importance of the formwork system discussed above, could tragically affect the development of construction and the workers' safety.

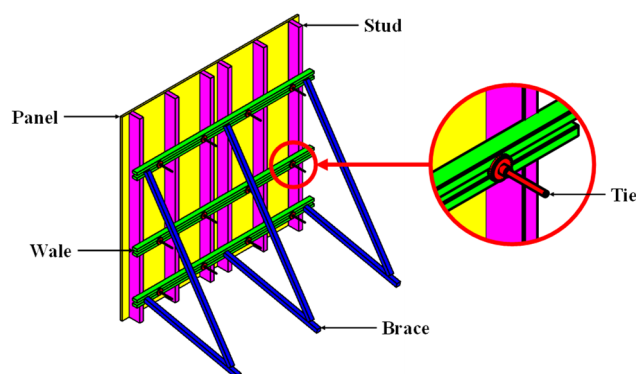


Figure 1. Typical formwork system and related members.

Other approaches, such as automatic measurement from 2D images or 3D point clouds, should be investigated to overcome the above shortcomings of the traditional spacing measurement. The spacing measurement from 2D images could result in greater accuracy errors, while 3D point clouds with higher accuracy would be a better candidate for this. A 3D point cloud is a set of data points containing three-dimensional Cartesian coordinates (X, Y, Z) and other information such as color (R, G, B) and reflectance or intensity. In this sense, construction site scenes can be rapidly reconstructed in terms of the 3D point cloud [9–11]. Specifically, the external surface of the formwork system can be effectively represented by data points in the 3D point cloud, and it is possible to automate the detection and measurement of different members in the formwork system using the three-dimensional Cartesian coordinates (X, Y, Z) contained in the data points [12]. For this reason, this research proposes a framework for the spacing measurement of formwork system members with 3D point cloud data. The aim of this paper is to contribute to the automation of the dimensional quality inspection process and present and test a framework within which to measure the spacing of the different members of the formwork system using 3D point cloud data in a non-human-reliant approach.

The rest of the paper is structured as follows. Section 2 reviews the literature on the acquisition approach of 3D point cloud data and its application for dimensional quality inspection in construction projects. Section 3 elaborates on the two parts with eight steps of the proposed framework, and a case study is conducted for its demonstration in Section 4. Section 5 discusses the findings from the case study and explores the significance of the proposed framework. In Section 6, the conclusion and outlook are provided.

2. Literature Review

This section gives an overview of the state of the art with respect to different approaches available for 3D point cloud data acquisition and the application of 3D point cloud data for dimensional quality inspection in construction projects.

2.1. Acquisition Approach of 3D Point Cloud Data

3D point cloud data can be acquired through various approaches, including laser scanning, photogrammetry, and videogrammetry [13]. Laser scanning is an approach to obtaining object information according to dense points detected by reflected laser beams [14]. In laser scanning, time-of-flight (ToF) and phase-shift (PS) are the main techniques for range measurement [15]. ToF uses the time interval between emitting and receiving a laser beam and the velocity of the laser to estimate the distance. PS applies the phase difference between emitting and receiving a laser beam and the wavelength of the laser to infer the distance. Photogrammetry is an approach to obtaining object information according to photographic images and patterns of electromagnetic radiant energy and other phenomena [16]. In photogrammetry, structure from motion (SfM) and multi-view stereo (MVS) are the primary methods for point cloud generation [15]. SfM matches feature points extracted from images to perform a sparse 3D reconstruction. MVS corrects images according to camera parameters output from SfM and matches feature points extracted from the images to perform a dense 3D reconstruction. Videogrammetry is an approach similar to photogrammetry but obtains object information from video streams [13]. In videogrammetry, the 3D reconstruction is determined by videos taken from different angles [15].

Generally, laser scanning has a higher measurement accuracy, a longer measurement range, less chance for user errors, and is not affected by lighting, whereas photogrammetry and videogrammetry have a lower cost and better visual representation of textures [17]. Since the installation quality of the formwork system is significantly related to the spacing of members, there is a relatively high requirement for the accuracy of the spacing measurement in construction projects. Meanwhile, the dynamic and complex nature of construction sites increases the uncertainty in the spacing measurement, requiring the data acquisition process to be more flexible and robust. In addition, the installation of the formwork system typically takes place outdoors; therefore, the data acquisition process is extremely susceptible to the influence of lighting. Keeping these points in mind, laser scanning is used for this research because it is more in line with the requirements and characteristics of the spacing measurement of formwork system members.

2.2. Dimensional Quality Inspection with 3D Point Cloud Data

3D point cloud data have been effectively applied to various dimensional quality inspections in construction projects. Some of the most relevant applications are summarized in terms of field, object, and inspection item in Table 1.

Precast components have become one of the most concerned fields with increasing demands on dimensional quality control during the fabrication stage, mainly involving objects such as reinforcing bars, concrete slabs and panels, and bridge deck slabs and girders. For reinforced precast components, reinforcing bars at connections significantly impact overall structural integrity. To guarantee that reinforcing bars are installed at the intended positions, a colored-point-cloud-based approach was provided to examine reinforcing bar positions [18]. The connection between precast components relies on reinforcing bars and sleeve ports. A methodology was presented to determine reinforcing bar sizes and positions and sleeve port sizes and positions for ensuring a successful connection [19]. Concrete slabs and panels are commonly used precast components, and they would cause structural failure if dimensional quality is not properly controlled. For assessing the dimensional quality of concrete slabs and panels, some methods were proposed to estimate slab and panel sizes and squareness as well as shear pocket sizes and positions [20,21]. Openings in the precast components increase the difficulty of dimensional quality control. A technique was presented by Kim et al. [22] to accelerate the inspection process in these cases to detect

panel sizes and squareness as well as hole sizes and positions. Shu et al. [23] proposed a method for examining the sizes and spacing of reinforcing bars, as well as the sizes of precast concrete elements (columns, beams, slabs, and walls) using deep-learning-based point cloud processing algorithms.

Table 1. Application of 3D point cloud data for dimensional quality inspection in construction projects.

Source	Field	Object	Inspection Item
[18]	Precast components	Reinforcing bars	Reinforcing bar positions
[19]		Reinforcing bars; sleeve ports	Reinforcing bar sizes and positions; sleeve port sizes and positions
[20]		Concrete slabs	Slab sizes; shear pocket sizes and positions
[21]		Concrete panels	Panel sizes and squareness; shear pocket sizes and positions
[22]		Concrete panels	Panel sizes and squareness; hole sizes and positions
[23]		Reinforcing bars; concrete columns, beams, slabs, and walls	Reinforcing bar sizes and spacing; column, beam, slab, and wall sizes
[24]		Bridge deck slabs; bridge girders	Shear pocket sizes and positions; shear connector orientations and positions
[25]		Bridge deck slabs	Panel depth; shear key sizes and positions; flat duct positions
[26]		Bridge deck slabs	Outer sizes; shear key sizes
[27]		Reinforced concrete components	Reinforcing bars; formwork
[28]	Reinforcing bars		Reinforcing bar sizes and spacing
[29]	Reinforcing bars		Reinforcing bar spacing
[30]	Steel structure components	Steel columns	Column positions and altitudes
[31]	Spatial structure components	Free-form structure elements	Element distance and torsion errors
[32]	Temporary structure components	Scaffolding platforms	Toe-board heights; guardrail positions
[33]		Formwork supporting frames	Pole positions and spacing; tube positions, heights and spacing; diagonal bracing positions

Precast bridge deck slabs and girders are widely used in bridge construction, and they are connected through shear pockets on deck slabs and shear connectors on girders. Yoon et al. [24] proposed a method to ensure the proper connection between bridge deck slabs and girders by checking shear pocket sizes and positions and shear connector orientations and positions. Considering that irregular precast components can increase the complexity of dimensional quality inspection, an approach was developed to assess the panel depth, shear key sizes and positions, and flat duct positions of a bridge deck slab with geometric irregularities [25]. The space for dimensional quality inspection is usually limited due to the close placement of precast components. Therefore, a mirror-aided methodology was proposed to estimate the outer sizes and shear key sizes of the side surface of a bridge deck slab [26].

Other components have also received attention, including those for reinforced concrete, steel structures, spatial structures, and temporary structures. The quality of reinforced concrete components depends largely on the correct installation of reinforcing bars and formwork. To monitor the placement of reinforcing bars in formwork, a method was designed to detect reinforcing bar spacing, concrete covers, and formwork inner sizes [27]. Since the bearing capacity of reinforced concrete components depends on the diameter and position of reinforcing bars, a methodology was proposed to classify reinforcing bar sizes and estimate reinforcing bar spacing [28], and an approach was presented to assess reinforcing bar spacing [29]. Taking into account the inadequacy of as-built dimension tracking solutions, a technique was proposed to examine the bottom and top center point positions and altitudes of steel columns for dimensional compliance control [30]. To enhance

the quality control accuracy and efficiency of complex spatial structure components, a method was developed to detect the distance and torsion errors of free-form structure elements [31]. For fall prevention systems used to ensure the safety of a scaffolding platform, a methodology was developed to evaluate the toe-board heights and guardrail positions to meet scaffolding safety regulations [32]. To reduce safety risks related to the improper installation of formwork supporting frames, an approach was presented to estimate pole positions and spacing, tube positions, heights and spacing, and diagonal bracing positions to comply with design requirements [33].

Overall, many dimensional quality inspections in construction projects have been beneficially explored with 3D point cloud data. However, the spacing measurement of formwork system members has received little attention. Formwork systems are different from the previously studied objects mentioned above (e.g., reinforcing bars, concrete slabs, steel columns, scaffolding platforms). There are specific force transfer features, material properties, and design standards for the formwork system, and it has unique members and layouts. A typical formwork system is composed of panels, studs, wales, ties, and braces that are installed following a fixed relative position order (Figure 1), which makes it difficult for previous studies to be applied to such members and layouts. Therefore, a specific methodology for the spacing measurement of formwork system members using 3D point cloud data needs to be developed. In particular, considering the purpose of enhancing the automation of the spacing measurement of formwork system members, it is essential and meaningful to conduct a specialized study for the segmentation, identification, and recognition of members according to the characteristics of the formwork system.

3. Proposed Framework

This section elaborates on the proposed framework for the spacing measurement of formwork system members with 3D point cloud data. This research focuses on the preprocessing, processing, and analysis of 3D point cloud data; therefore, the data acquisition process is out of our scope (i.e., 3D point cloud data have already been obtained). The proposed framework is divided into two parts: (1) 3D point cloud data preprocessing and (2) 3D point cloud data processing and analysis (Figure 2). Each part is detailed below.

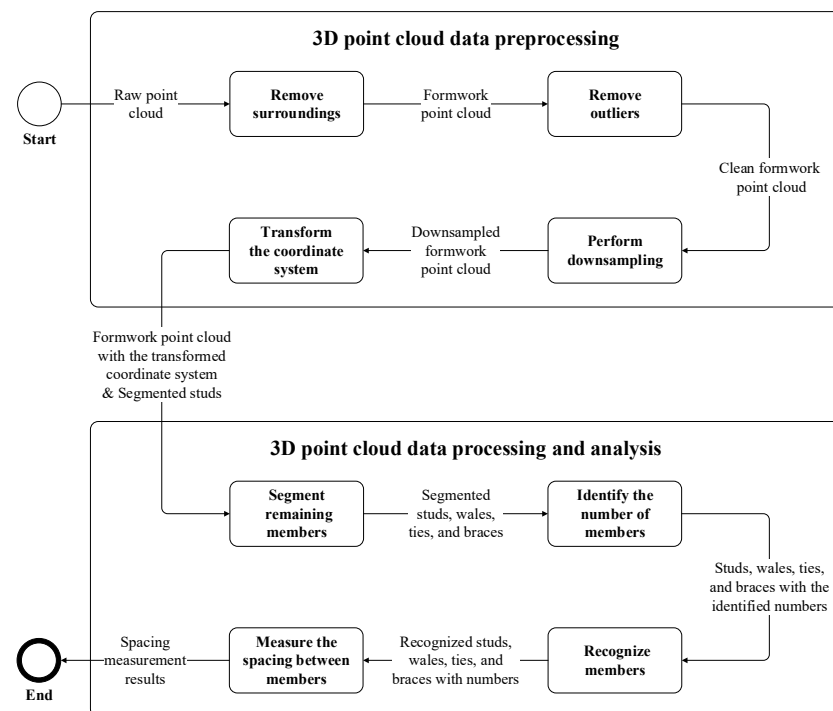


Figure 2. Proposed framework for the spacing measurement of formwork system members with 3D point cloud data.

3.1. 3D Point Cloud Data Preprocessing

The collected raw data need to be preprocessed for further use. Key steps include the removal of surrounding points that are out of the scope element (i.e., the formwork system), the removal of outliers that could affect the performance of the dimensional quality inspection, performing downsampling to alleviate the computing requirements, and finally, transforming the coordinate system of the resulting point cloud.

3.1.1. Remove Surroundings

The first step is to remove the surroundings around the formwork system to avoid interfering with the spacing measurement. The point cloud acquired via laser scanning typically contains not only information on formwork system members but also on all surroundings due to the larger range of laser scanners (over 100 m in most cases). The surroundings are of no use for the spacing measurement and should be removed, including the formwork panels that are not related to the spacing measurement, even though they are part of the formwork system.

Since the number of points that belong to the surroundings is generally substantial, a pass-through filter that enables fast filtering is applied to remove them. Through confirming the 3D coordinates of the studied formwork system within the point cloud, the desired points inside or outside the set threshold of 3D coordinates are retained, and the other points are removed by the pass-through filter. The coordinates that act as thresholds for the pass-through filter are determined by manually extracting the corners of the studied formwork system in any point-cloud viewing software like CloudCompare [34].

In some cases, the ground is close to formwork system members, which makes it difficult to be removed completely. Generally, the number of points that belong to the ground is significantly higher than that of formwork system members along the normal direction of the ground. In other words, a histogram of the number of points along the Z-axis of the point cloud has different peaks. The highest peak in the histogram would represent the ground level (i.e., a higher number of points), and it can be easily distinguished from lower peaks representing the formwork system members close to the ground (i.e., a lower number of points), which is also an advantage compared to other point cloud fitting techniques, such as the random sample consensus algorithm (RANSAC) that needs to know which plane represents the ground. For this reason, the single-peak detection algorithm can be applied to remove the ground. To generalize this and consider the cases when other elements are close to the ground (e.g., clutter or other materials on the ground next to the formwork system members), the bin interval can be adjusted to include the points of these elements depending on the type of conditions investigated. For example, when the bin interval is set to 1 dm, the second-highest peak representing the undesired elements would not be removed by the single-peak detection algorithm (Figure 3a). When the bin interval is adjusted to 2 dm, those undesired elements are placed at the highest peak (Figure 3b); thus, they can be removed successfully.

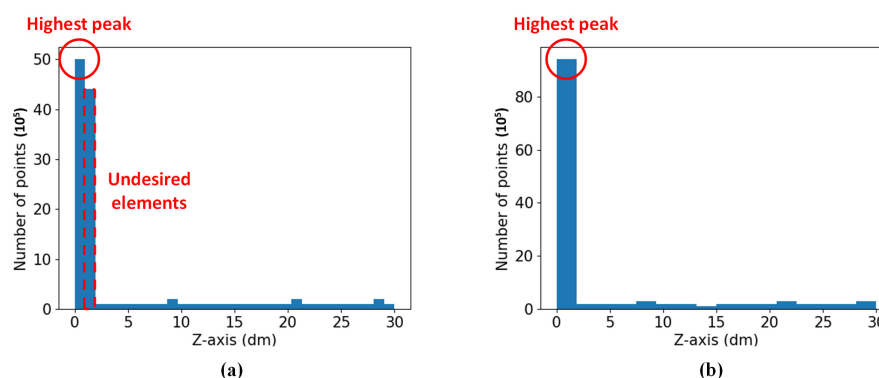


Figure 3. Adjustment of the bin interval for removing undesired elements close to the ground (the bin interval is 1 dm (a) or 2 dm (b)).

3.1.2. Remove Outliers

The second step is to remove the point cloud outliers that can adversely affect the spacing measurement of formwork system members. Laser scanning often produces point cloud outliers due to the presence of highly reflective surfaces, see-through objects, or around sharp corners where laser beams do not reflect properly. Although the number of point cloud outliers is not large compared to the total number of points, point cloud outliers can complicate data processing and analysis and generate erroneous values. This may lead to the failure of the spacing measurement of formwork system members, on top of increasing the computational time and resources required to process points that do not add any semantic value.

Considering that point cloud outliers are featured by being sparsely distributed in space, the statistical outlier removal approach [35], based on the computation of the distribution of distances between points and their neighbors, is employed to remove point cloud outliers. For each point, the mean distance to the set number of nearest neighbors is computed. The resulting mean distances of all points are assumed to follow a Gaussian distribution. If the mean distance of a point is outside the interval defined by the mean and the standard deviation of the Gaussian distribution, it is considered an outlier and removed from the point cloud.

3.1.3. Perform Downsampling

The third step is to perform the downsampling of the point cloud to further reduce computational effort and errors. Laser scanning may produce overly dense and unevenly distributed point clouds, which can burden data processing and mislead data analysis, and is not conducive to the spacing measurement of formwork system members.

To mitigate such negative effects, a voxel grid filter that enables downsampling is utilized to decrease the density of the point cloud and make the distribution of the point cloud more uniform. The voxel grid filter is chosen because it is able to remove duplicated and non-essential information while still maintaining a good amount of detail from the point cloud, in contrast with other point cloud downsampling techniques like random subsampling. By setting a voxel size, points that fall within the cubic voxel are replaced with a centroid point, approximately representing the replaced points, to reduce the density of the point cloud without losing important features.

It should be noted that the reason for performing downsampling after removing outliers is that the points of some small-sized formwork system members (e.g., ties) may be incorrectly classified as outliers due to the smaller number of points and thus removed if the order is reversed.

3.1.4. Transform the Coordinate System

The fourth step is to transform the coordinate system of the formwork system members so that it can facilitate the spacing measurement. The coordinate system of the point cloud acquired via laser scanning usually does not adapt well to the orientation of formwork system members, which complicates the process of segmentation, identification, and recognition. Since formwork system members always follow a set of specific orientations, the process can be simplified if the coordinate system of the point cloud is aligned with those orientations.

For the transformation of the coordinate system, the front surface of a stud with a rectangular shape feature is a suitable reference because its long sides are significantly longer than its short sides; thus, the orientation of the transformed coordinate system is easy to identify. The plane corresponding to the front surface of all studs is the one with the maximum number of points (compared to the other mostly occluded planes of the members), and RANSAC is applied for plane fitting [36]. RANSAC is widely used for robust parameter estimation in the presence of a significant fraction of outliers in the data. Random points are selected to form a plane (Figure 4a) where the offset of points around the estimated plane are computed across several iterations until most of the points

in the neighborhood are within the set threshold (t) (Figure 4b). The fitted plane is used to segment the front surface of all studs first (Figure 5a). The rest of the members do not need to be segmented since the front surface is enough to further perform measurements. Then, the RANSAC for line fitting [36] is applied to detect the front surface of a single stud in the detected front surface of all the studs (Figure 5b).

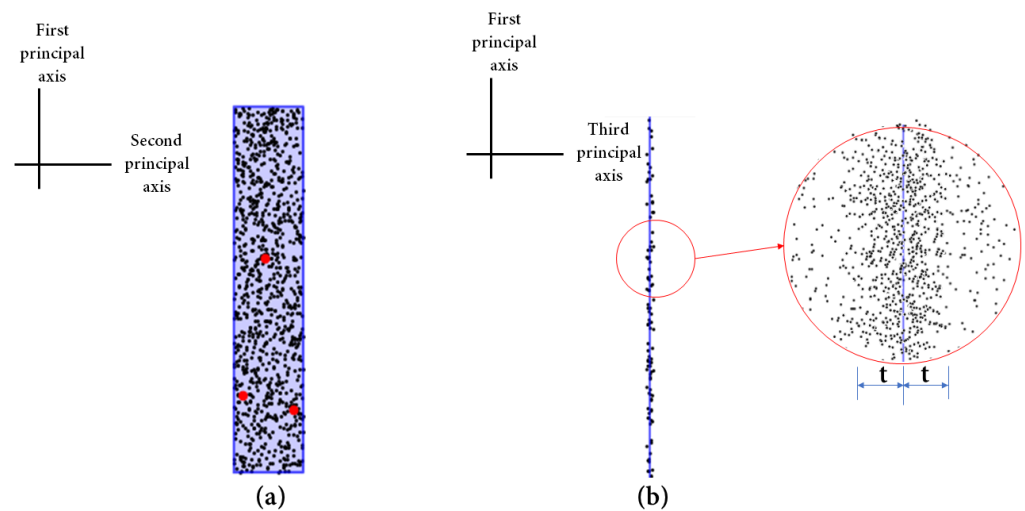


Figure 4. RANSAC for plane fitting: (a) three randomly selected points fitting a plane (highlighted in red); and (b) the threshold (t) representation.

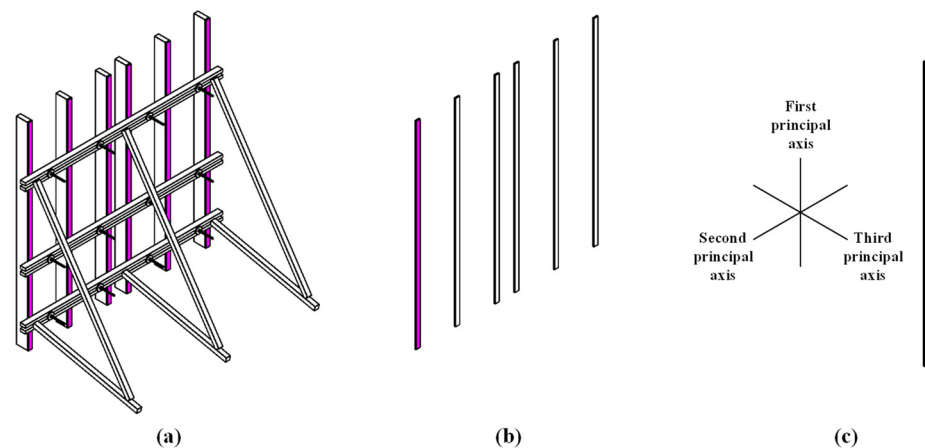


Figure 5. Transformation of the coordinate system of formwork system members: (a) detection of the front surface of all studs (highlighted in purple) applying the RANSAC for plane fitting; (b) detection of the front surface of a single stud (highlighted in purple) applying the RANSAC for line fitting; and (c) determination of the transformed coordinate system applying the PCA.

In order to determine the transformed coordinate system, the principal component analysis (PCA) is applied according to the detected stud front surface (Figure 5c). The first, second, and third principal axes of the transformed coordinate system correspond to the long side, short side, and normal directions of the detected stud front surface, respectively. With respect to the PCA [37], the first principal axis of the transformed coordinate system is determined so that the distribution variance of the projection of all the points of the detected stud front surface is maximized on this coordinate axis (i.e., the first principal component). The second principal axis is determined so that the distribution variance is maximized on the one that is orthogonal to the first coordinate axis (i.e., the second principal component). Finally, the last principal axis is the one orthogonal to the first and second principal axes (i.e., the third principal component).

3.2. 3D Point Cloud Data Processing and Analysis

During the 3D point cloud data processing and analysis, there are four steps: (1) segment remaining members; (2) identify the number of members; (3) recognize members; and (4) measure the spacing between members.

3.2.1. Segment Remaining Members

The first step is to segment the remaining categories of formwork system members based on the transformed coordinate system. Since studs have been segmented before transforming the coordinate system, only wales, ties, and braces need to be segmented in this step.

Various categories of formwork system members follow a well-defined force transfer path. The force that panels bear is transferred to studs, wales, ties, and braces, which are installed following a fixed relative position order along the third principal axis. For wales that do not overlap with ties and braces along the third principal axis, considering that the plane corresponding to the front surface of all wales is the one with the maximum number of points after removing the front surface of studs, the RANSAC for plane fitting is employed for its segmentation (Figure 6a). For ties and braces that overlap with each other along the third principal axis, they are segmented employing the density-based spatial clustering of applications with noise (DBSCAN) [38] (Figure 6b). Regarding the DBSCAN, in each cluster, points that meet a set minimum number of points within the set distance are identified as core points of a tie or brace first; then, points that are within the set distance of the core points are identified as border points of the tie or brace; otherwise, they are identified as outliers of the tie or brace [4].

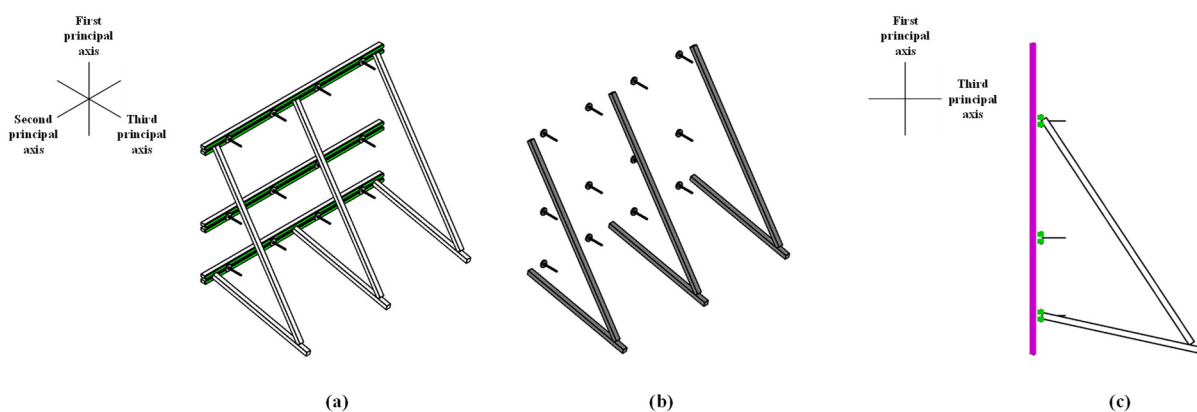


Figure 6. Segmentation of different categories of formwork system members: (a) detection of the front surface of wales (highlighted in green) employing the RANSAC for plane fitting; (b) detection of ties and braces (all highlighted in gray as they are unknown categories by the current step) employing the DBSCAN; and (c) identification of the direction of the third principal axis comparing studs (highlighted in purple) and wales (highlighted in green) from the side view.

To facilitate the segmentation of ties and braces, the direction of the third principal axis required for removing the points that belong to other formwork system members (i.e., whether the points lie in the positive or negative direction of the axis) needs to be identified. Since formwork system members are installed in turn along the same direction of the third principal axis, the mean values of the coordinates of the points of the detected front surfaces for the stud and wale on the third principal axis are compared and used to identify the axis direction (Figure 6c). For example, if the mean value of the coordinates of points of the detected front surface for the stud (highlighted in purple) is smaller than that for the wale (highlighted in green), it implies that formwork system members are installed along the positive direction of the third principal axis; otherwise, they are along the negative direction of the third principal axis.

3.2.2. Identify the Number of Members

The second step is to identify the number of formwork system members in each category. Various categories of formwork system members have specific layouts. Formwork system members such as studs are installed along the second principal axis (Figure 7a), and formwork system members such as wales are installed along the first principal axis (Figure 7b). In other words, for a category of formwork system members that are installed along a specific principal axis, when creating a histogram of the number of points along this principal axis, a peak in the histogram represents a formwork system member, and it can be easily distinguished from lower peaks representing member spacing beside it.

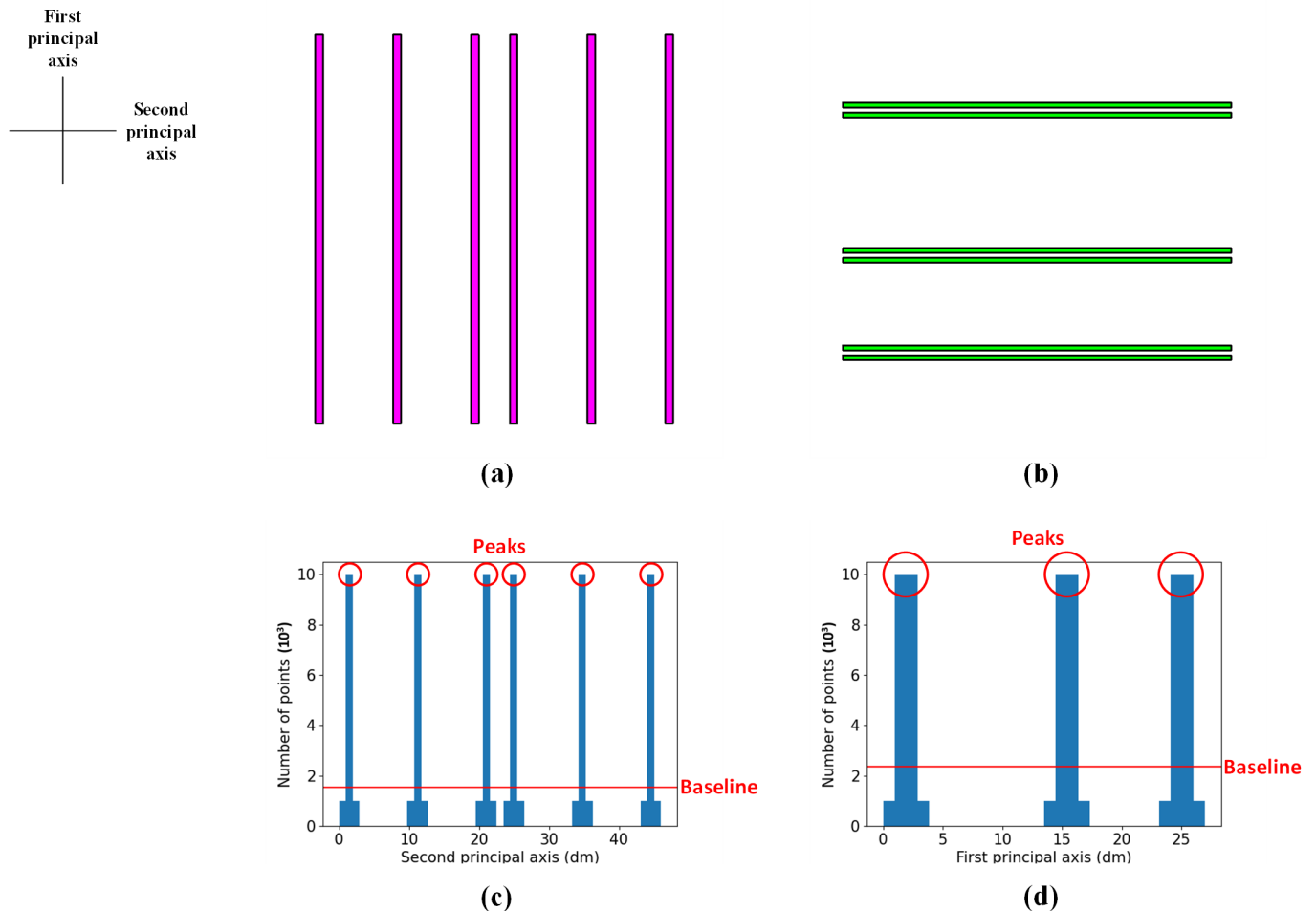


Figure 7. Installation layouts of studs (a) and wales (b) from the front view and identification of the number of studs (c) and wales (d) utilizing the multiple peak detection algorithm.

Considering such characteristics, the multiple-peak detection algorithm is utilized to identify the number of studs and wales because they have been previously segmented into different sets of points with all formwork system members in their respective categories. For the multiple-peak detection algorithm, the number of points for studs or wales is averaged into a baseline over the range of the second or first principal axis, and the number of points in each set bin is counted sequentially. If the number of points first exceeds and then falls below the baseline, it is considered a stud or wale (Figure 7c,d). The numbers of studs and wales are identified utilizing the multiple-peak detection algorithm instead of other point cloud clustering techniques, such as DBSCAN, because the points that belong to a stud or wale, occluded by other formwork system members, are separated and cannot be clustered well.

Although ties and braces have been previously segmented into different sets of points with a single formwork system member, it is unknown to which category a set of points

belongs. Since the number of points for a tie is significantly smaller than that for a brace, the point number comparison algorithm is utilized to identify the number of ties and braces. For the point number comparison algorithm, the number of points for ties and braces is averaged into a baseline over the total number of ties and braces, and the number of points for each tie and brace is counted sequentially. If the number of points for a formwork system member is smaller than the baseline, it is considered a tie; otherwise, it is considered a brace.

3.2.3. Recognize Members

The third step is to recognize the formwork system members in each category. To facilitate the spacing measurement and the corresponding result positioning, each formwork system member in the same category needs to be detected and numbered.

Although the positions of studs, braces, and wales can be approximately estimated with the histogram from the previous step, it is not accurate enough. Thus, the RANSAC for line fitting is applied to detect each formwork system member, and a brace is required to be particularly detected twice as it consists of two poles. Since a category of formwork system members is installed along a specific principal axis, the relative position of each member can be determined according to the mean value of the coordinates of its points on this principal axis when compared to those of other members in the same category. In this sense, formwork system members in each category are numbered sequentially in ascending order of mean values for recognition. This process stops when the corresponding identified number is reached.

For studs and braces installed along the second principal axis, the stud or brace with the smallest mean value on the second principal axis among its same category is located on the leftmost or rightmost from the front view and is numbered “1”. The stud or brace with the second smallest mean value is located immediately to the right or left of it and is numbered “2”, and the rest of the studs or braces can be deduced by analogy (Figure 8a,b).

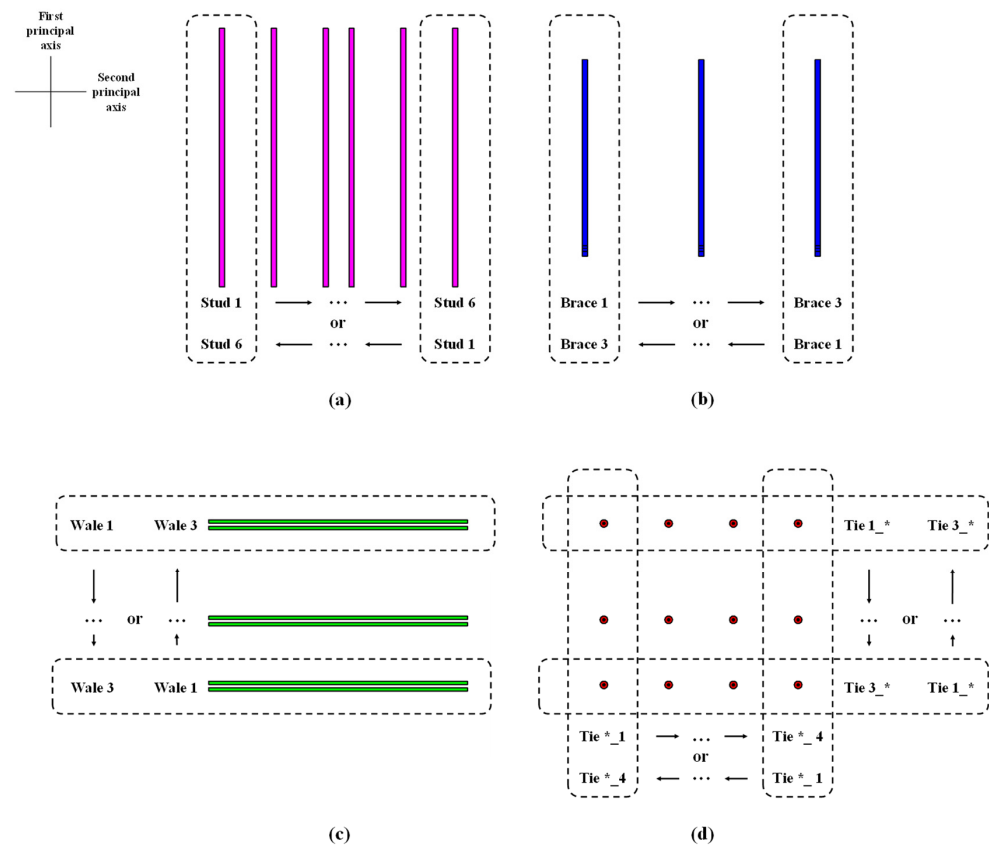


Figure 8. Recognition of studs (a), braces (b), wales (c), and ties (d) from the front view.

For wales that are installed along the first principal axis, the wale with the smallest mean value on the first principal axis among its same category is located on the bottommost or topmost from the front view and is numbered “1”. The brace with the second smallest mean value is located immediately to the top or bottom of it and is numbered “2”, and the rest of the wales can be deduced by analogy (Figure 8c).

For ties that are not solely installed along the first or second principal axis, they are grouped depending on whether mean values are within the range of the wale numbered “1” on the first principal axis. The tie with the smallest mean value on the second principal axis in the first group is located on the leftmost or rightmost from the front view and is numbered “1_1”. The tie with the second smallest mean value in the first group is located immediately to the right or left of it and is numbered “1_2”, and the rest of the ties in the first group can be deduced by analogy. Similarly, ties outside the first group are numbered sequentially as above (i.e., 2_1, 2_2, . . . , 3_1, 3_2, . . .) (Figure 8d).

3.2.4. Measure the Spacing between Members

The fourth step is to measure the spacing between formwork system members in each category. For studs and braces that are installed along the second principal axis, the spacing to be measured corresponds to the horizontal spacing from the front view (Figure 9a,b). For wales that are installed along the first principal axis, the spacing to be measured corresponds to the vertical spacing from the front view (Figure 9c). For ties that are not solely installed along the first or second principal axis, the spacing to be measured corresponds to the horizontal spacing from the front view because their vertical spacing has been controlled by wales (Figure 9d).

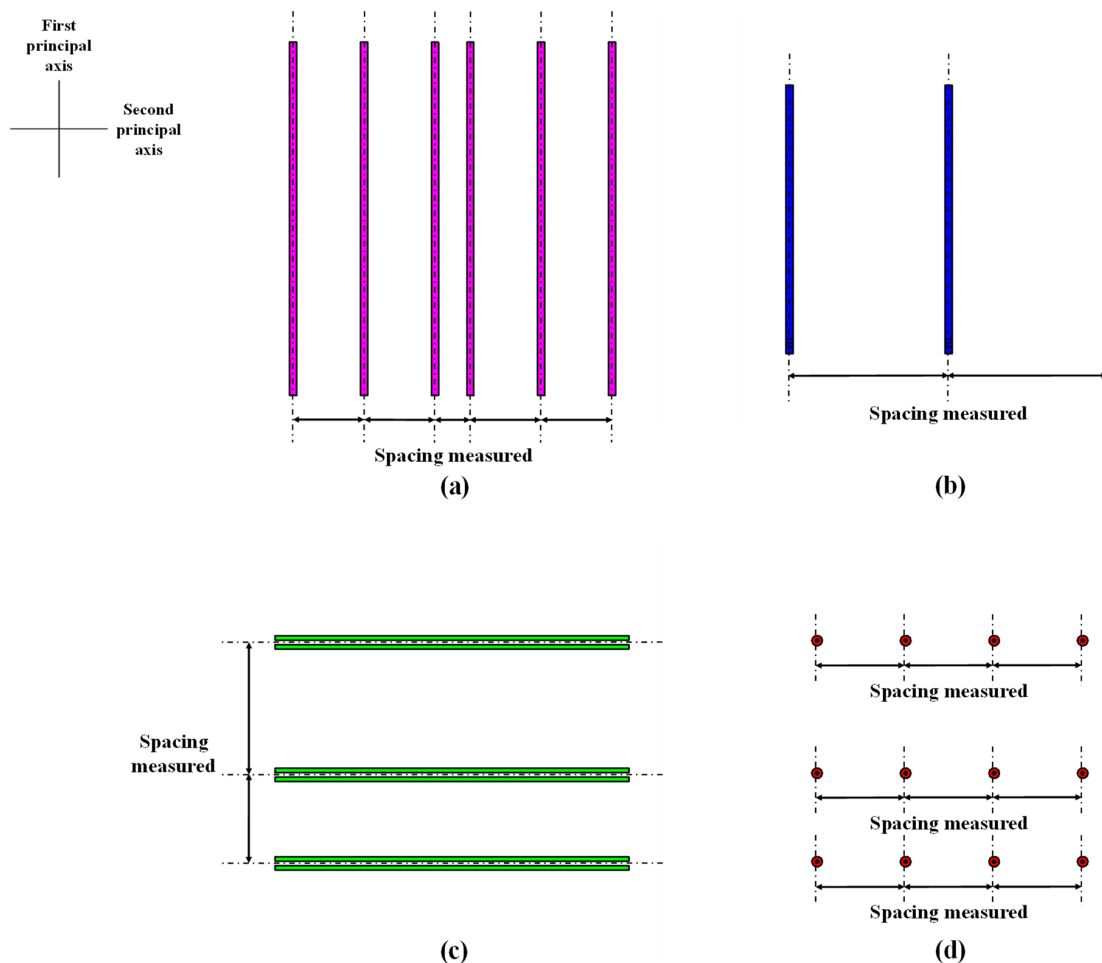


Figure 9. Spacing measurement of studs (a), braces (b), wales (c), and ties (d) from the front view.

In each category of formwork system members, spacing is determined by the difference between the mean values of the coordinates of points of two adjacently numbered members on the corresponding principal axis. As a result, the mean values of studs, braces, and ties are derived from the coordinates of points on the second principal axis, and those of wales are derived from the coordinates of points on the first principal axis.

4. Case Study

A formwork system on an ongoing construction project on a university campus was used to demonstrate the feasibility and effectiveness of the proposed framework.

4.1. Data Collection

The data were collected with a 3D laser scanner (Figure 10a). The scanner used was a Leica BLK360 (Leica Geosystems, St. Gallen, Switzerland) with the specifications summarized in Table 2. It is able to collect geometric 3D information, reflectance information, RGB color information, and thermal information. Only the geometric 3D information is of interest for this particular case study.

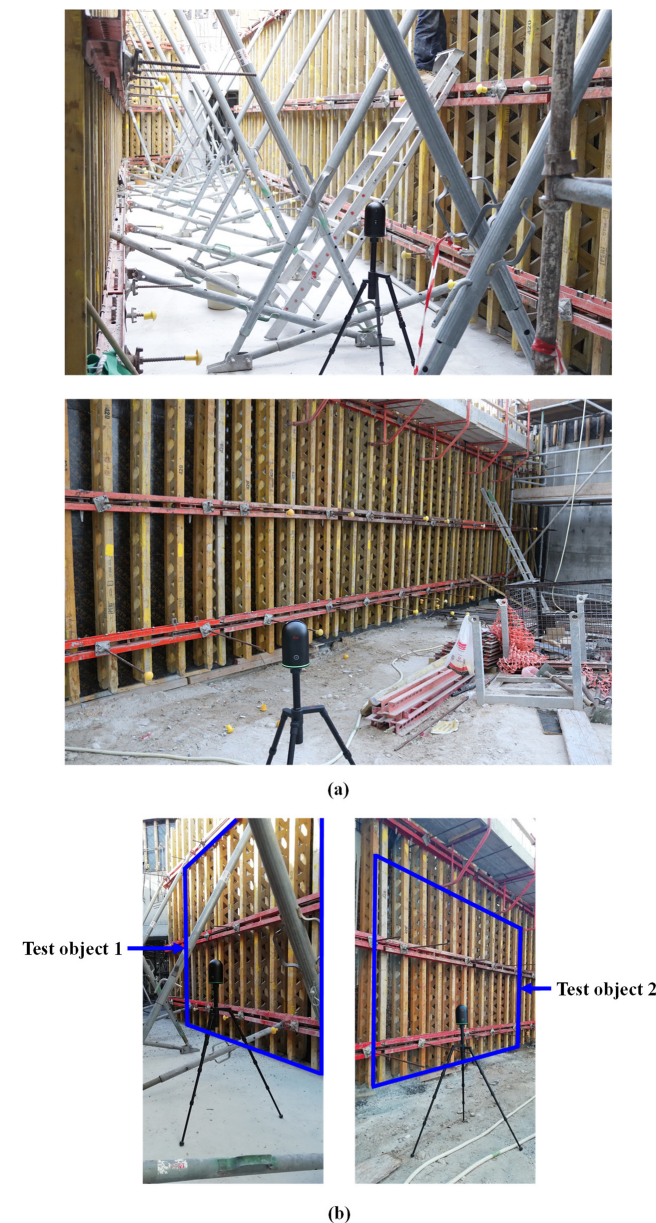


Figure 10. General overview of the studied formwork system (a) and detail of test objects 1 and 2 (b).

Table 2. Specifications of the Leica BLK360 3D scanner [39].

Specification	Value
Field of view (H × V)	360° × 300°
Scanning range [min, max]	[0.6 m, 60 m]
Point measurement rate	up to 360,000 pts/s
3D point accuracy	6 mm@10 m/8 mm@20 m

The test objects were two sections of the formwork system (Figure 10b). The first section (test object 1) included eleven studs, two wales, eight ties, and two braces. The second section (test object 2) included twelve studs, two wales, and eight ties. Test object 1 belonged to a narrow corridor, challenging the system with plenty of occlusions.

In order to compare spacing measurement results under different conditions, five cases were conducted with different test objects as well as numbers and distances of scans. The different parameters for the five cases are summarized in Table 3. Case 1 and Case 2, with different test objects, were used to verify the robustness of measurements. Case 2 and Case 3, with different numbers of scans, were used to verify the impact of the number on measurements. Case 3, Case 4, and Case 5, with different distances of scans, were used to verify the impact of the distance on measurements.

Table 3. Characteristics of the five cases.

Case	Test Object	Number of Scans	Spacing of Scans (m) *	Distance of Scans (m) **
1	1	2	4.0	1.5
2	2	2	4.0	1.5
3	2	1	-	1.5
4	2	1	-	3.0
5	2	1	-	4.5

* Spacing in between locations of scanning positions. ** Distance from the laser scanner to the test object measured perpendicularly.

There are several effective libraries for processing the acquired 3D point cloud data, including Trimesh [40], PyTorch3D [41], Open3D [42], and OpenSFM [43], all of them using Python. There are also Point Cloud Library (PCL) [44] and Point Data Abstraction Library (PDAL) [45], both using C++ as the primary language. Benchmarking the different available libraries is out of the scope of this case study. For the case study, Open3D Version 0.15 was used.

All the values for the different parameters used in the algorithms were chosen based on experimentation, settling down for those that achieved the best results. Case 1 is used as an example to display the details of the test, and the process for the other cases is similar. The results of all the tests are presented numerically.

4.2. 3D Point Cloud Data Preprocessing

In the first part, 3D point cloud data were preprocessed, as shown in Figure 11.

First, the surroundings of the formwork system were removed from the raw point cloud (Figure 11a). The thresholds of the pass-through filter were set according to the coordinates of points for the formwork system viewed on CloudCompare Version v2.12.2 [34], and the raw point cloud was filtered to the desired portion (Figure 11b). To remove the ground, the number of points in each bin with an interval of 0.05 m was counted on the Z-axis of the histogram. The highest peak was considered as the ground level (Figure 11c), and the points on the ground level and below were removed (Figure 11d).

Next, the outliers marked in red were removed from the point cloud (Figure 11e). For the removal of the outliers, 100 neighbors were considered for computing the average distance for a given point, and the threshold based on the standard deviation of the average distances was set to 1.

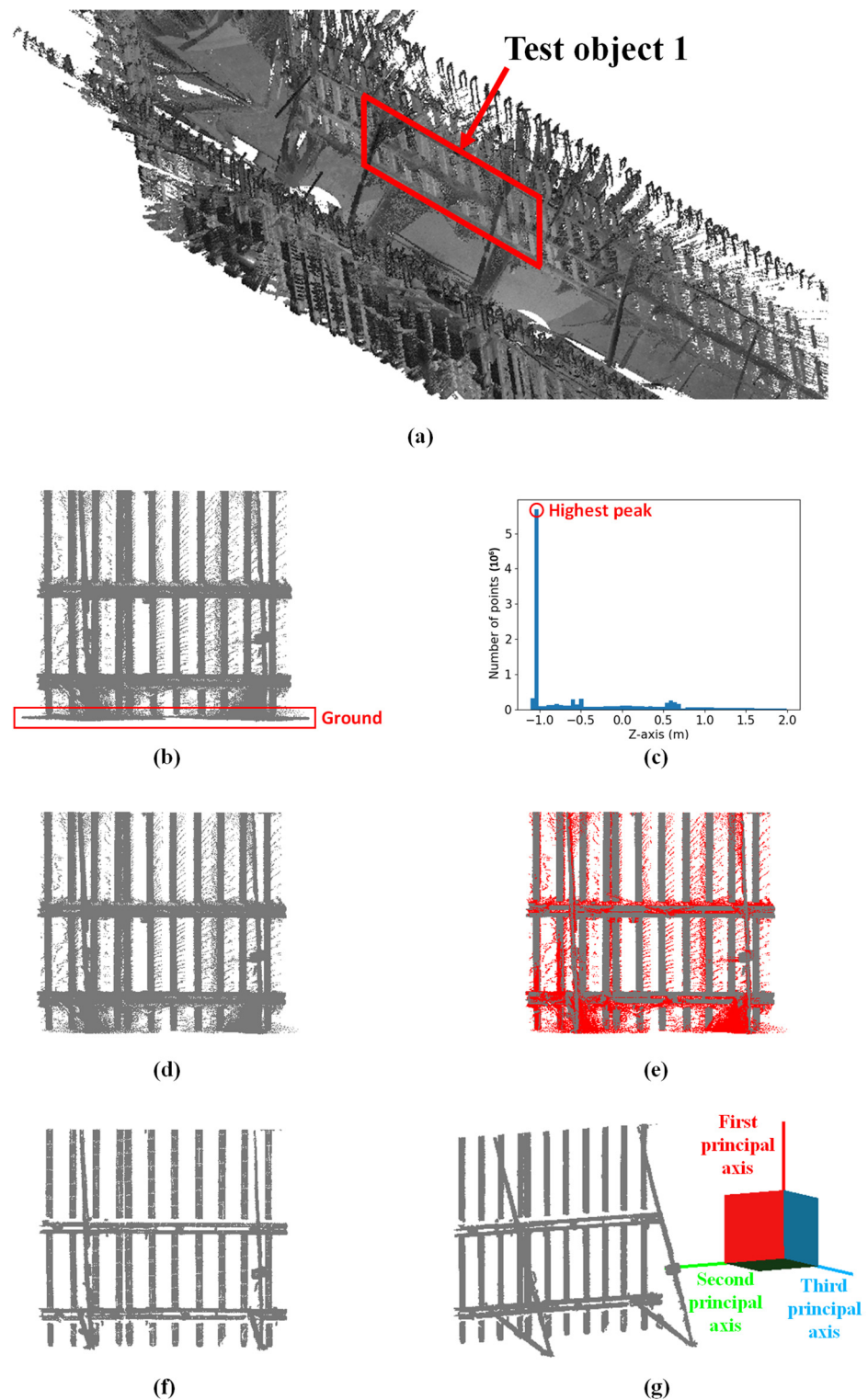


Figure 11. 3D point cloud data preprocessing: (a) the raw point cloud; (b) the point cloud after removing the surroundings except for the ground; (c) the histogram of the number of points for the point cloud on the Z-axis; (d) the point cloud after removing the ground; (e) the point cloud after removing the outliers (highlighted in red); (f) the point cloud after performing downsampling; and (g) the point cloud after transforming the coordinate system.

Then, the downsampling of the point cloud was performed by setting a voxel size of 0.01 m (Figure 11f).

Finally, the studs were segmented, and the coordinate system of the point cloud was transformed (Figure 11g). The first, second, and third principal axes of the transformed coordinate system were the long side, short side, and normal directions of the detected stud surface, respectively. The RANSAC for plane fitting was applied to segment the front surface of the studs. In this case, the RANSAC for plane fitting was implemented by setting the distance threshold (t) as 0.01 m and randomly selecting three points (Figure 4). The process of verifying a randomly sampled plane was repeated 1000 times.

4.3. 3D Point Cloud Data Processing and Analysis

In the second part, 3D point cloud data were processed and analyzed, as shown in Figure 12.

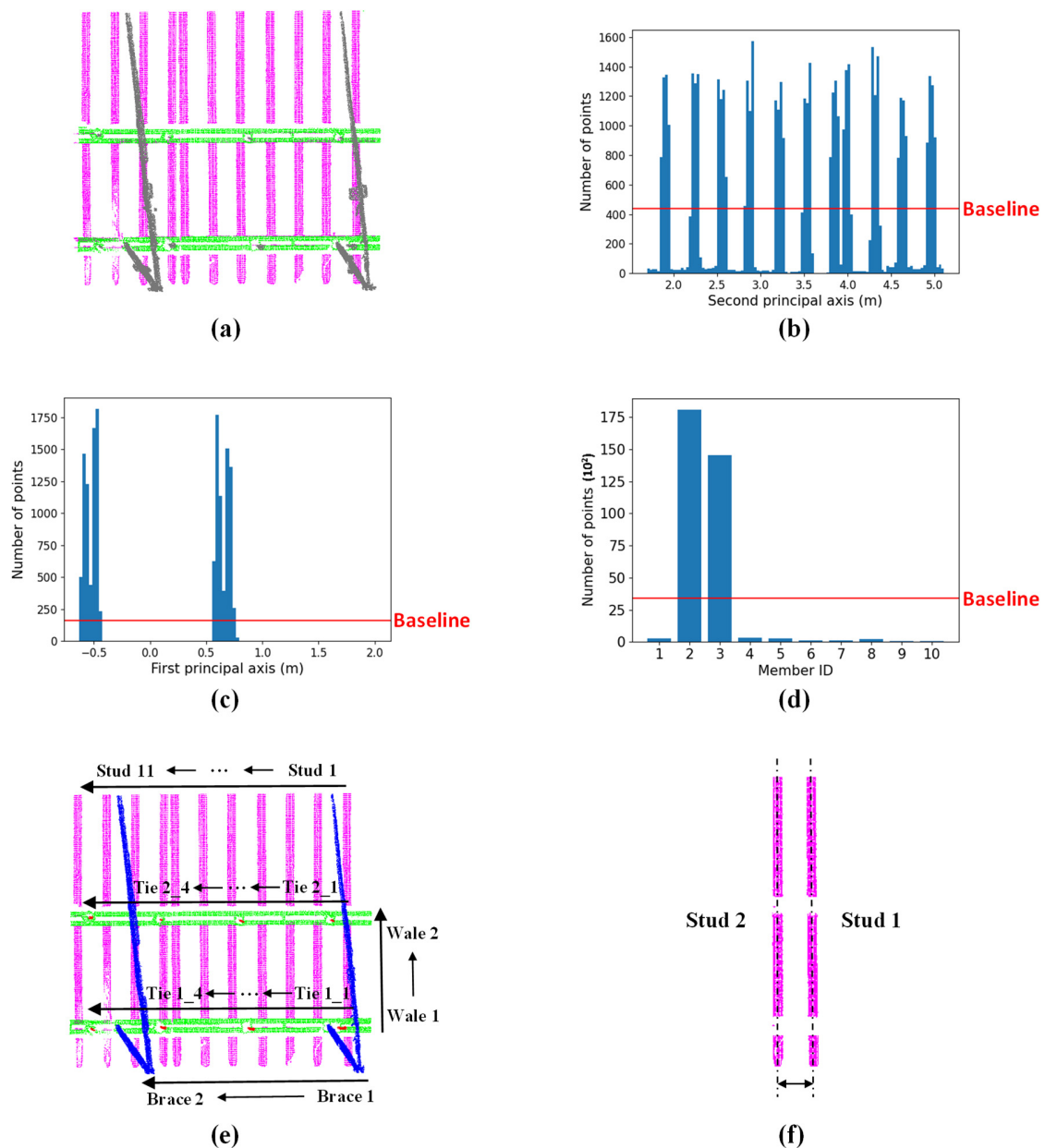


Figure 12. 3D point cloud data processing and analysis: (a) the segmentation of the different categories of formwork system members; (b) the histogram of the number of points for the studs on the second principal axis; (c) the histogram of the number of points for the wales on the first principal axis; (d) the histogram of the number of points for the ties and braces; (e) the recognition of the formwork system members in each category; and (f) the spacing between Stud 1 and Stud 2.

First, the remaining categories of formwork system members were segmented based on the newly transformed coordinate system (Figure 12a). The points marked in purple, green, and gray represent the segmented studs (vertical elements), wales (horizontal elements), and ties and braces, respectively. To segment the front surface of the wales with the RANSAC for plane fitting, the distance threshold was set as 0.01 m, three points were randomly sampled, and the process of verifying a randomly sampled plane was repeated 1000 times. DBSCAN was applied to segment the ties and the braces. For the DBSCAN parameters, the distance to neighbors within a cluster was established at 0.05 m, with a requirement of at least 30 points to form a valid cluster.

Next, the number of the formwork system members in each category were identified. The number of the studs was determined using the multiple-peak detection algorithm along the second principal axis. As shown in Figure 12b, the baseline passes through eleven distinct peaks in the histogram, which led to eleven studs. Similarly, the number of wales was determined by applying the multiple-peak detection method along the first principal axis. As shown in Figure 12c, the baseline passes through two distinct peaks in the histogram, which led to two wales. The number of points for the ties and braces was counted, and eight ties and two braces were identified according to the baseline determined by the average number of the points over their total number (i.e., ten) (Figure 12d).

Then, the formwork system members in each category were recognized (Figure 12e). The studs and the braces were numbered in consecutive sequence along the second principal axis. This was achieved by arranging the mean values of the coordinates of points for each stud and brace sequentially, from smallest to largest (i.e., Stud 1, . . . , and Stud 11; Brace 1 and Brace 2). Similarly, the wales were numbered in consecutive sequence along the first principal axis from smallest to largest (i.e., Wale 1 and Wale 2). On the other hand, the ties were numbered by considering the mean values of the coordinates of points on both the first and second principal axes from smallest to largest (i.e., Tie 1_1, . . . , Tie 1_4, Tie 2_1, . . . , and Tie 2_4).

Finally, with all the formwork system members properly recognized, the spacing can be measured by computing the distance between two adjacently numbered members from the same category. This distance is equivalent to the shortest perpendicular distance between the centers of each member. For example (Figure 12f), the spacing between Stud 1 and Stud 2 was the difference between the mean values of the coordinates of their points on the second principal axis.

5. Results and Discussion

The spacing measurement results are summarized in Table 4. They show the relative performance (i.e., the difference) of the 3D point cloud data approach (R^{pc}) and the manual approach with the traditional measuring tools (i.e., measuring tape and laser distance meter) (R^{mt}) in terms of the mean absolute error (MAE) (Equation (1)) and the mean absolute percentage error (MAPE) (Equation (2)):

$$\text{MAE} = \frac{1}{n} \sum_{i=1}^n |R_i^{pc} - R_i^{mt}|, \quad (1)$$

$$\text{MAPE} = \frac{100\%}{n} \sum_{i=1}^n \left| \frac{R_i^{pc} - R_i^{mt}}{R_i^{mt}} \right|. \quad (2)$$

The MAE and the MAPE for each category of formwork system members were calculated for the five cases. For instance, in Case 1, the minimum and maximum MAEs were from the wale and the brace, respectively, and the minimum and maximum MAPEs were from the wale and the tie, respectively.

In terms of cases, the minimum and maximum MAEs for all formwork system members correspond to Case 4 and Case 5, respectively, and the minimum and maximum MAPEs for all formwork system members were also from Case 4 and Case 5, respectively. This shows that the measurements were optimal when they were taken from a distance of

3 m (Case 4), proving that if the measurements were taken too close (Case 3), the number of occlusions was not beneficial for the analysis, and if the measurements were taken too far (Case 5), the performance was also affected. In terms of formwork system members, the minimum and maximum MAEs for all cases were from the wale and the brace, respectively, and the minimum and maximum MAPEs for all cases were from the wale and the stud, respectively. The poor performance of the brace in Case 1 was caused due to the presence of occlusions, given that the data were collected in a narrow corridor.

Table 4. Relative performance of the 3D point cloud data approach and the manual approach in terms of MAE and MAPE.

Formwork System Member	Metric	Case					
		1	2	3	4	5	All **
Stud	MAE (mm)	1.60	1.64	2.45	1.36	2.09	1.83
	MAPE (%)	0.49	0.52	0.78	0.45	0.69	0.59
Wale	MAE (mm)	1.00	1.00	2.00	2.00	3.00	1.80
	MAPE (%)	0.08	0.08	0.17	0.17	0.25	0.15
Tie	MAE (mm)	4.83	5.33	4.17	4.33	8.17	5.37
	MAPE (%)	0.52	0.55	0.40	0.45	0.86	0.55
Brace	MAE (mm)	11.00	-	-	-	-	11.00
	MAPE (%)	0.46	-	-	-	-	0.46
All *	MAE (mm)	3.17	2.83	3.00	2.39	4.17	3.11
	MAPE (%)	0.48	0.51	0.62	0.43	0.72	0.55

* Results for all formwork system members (Average). ** Results for all cases (Average).

Overall, the MAE and MAPE for all formwork system members in all cases were 3.11 mm and 0.55%, respectively.

The comparison of the spacing measurement results with error bars is shown in Figure 13. The means are represented by blue dots, and the means \pm standard deviation are represented by upper and lower red caps, respectively. The comparison of the stud, the wale, and the tie is shown in Figure 13a,b. The brace is removed from the comparison as there is only one result and, therefore, no variation. The performance of the wale was better whether in the MAE or the MAPE, and the performances of the tie and the stud were worse in the MAE and the MAPE, respectively. The reasons may be that (1) the wale was large in size and less occluded by other members, so the scanning effect was relatively good; (2) the tie was the smallest in size and made out of a higher reflective surface (i.e., metal), so the scanning presented less density and quality; thus, it performed relatively poorly in the MAE; and (3) the stud was not worst in the MAE but had a relatively poor performance in the MAPE due to its small spacing. The comparison of Case 1 and Case 2 with different test objects is shown in Figure 13c,d. The performances of the two cases were similar, indicating that the proposed approach was robust within the conditions of the tested cases. The comparison of Case 2 and Case 3 with different numbers of scans is shown in Figure 13e,f. The performance of Case 2 was slightly better than that of Case 3, suggesting that the increase in the number of scans was beneficial in improving the scanning effect (as expected). The comparison of Case 3, Case 4, and Case 5 with different distances of scans is shown in Figure 13g,h. The performance of Case 4 was better than that of the other two cases, and the performance of Case 5 was worse than that of Case 3, which suggested that the distance of scans should be moderate, and too far or too close was not good.

The proposed framework for measuring the spacing of formwork system members using 3D point cloud data has been evaluated using an experiment involving multiple cases under different conditions. The results demonstrated that the proposed framework is both feasible and effective. Considering the unique member and layout characteristics of the formwork system, the framework proposed the following three main contributions to enable a high degree of automation for the spacing measurement.

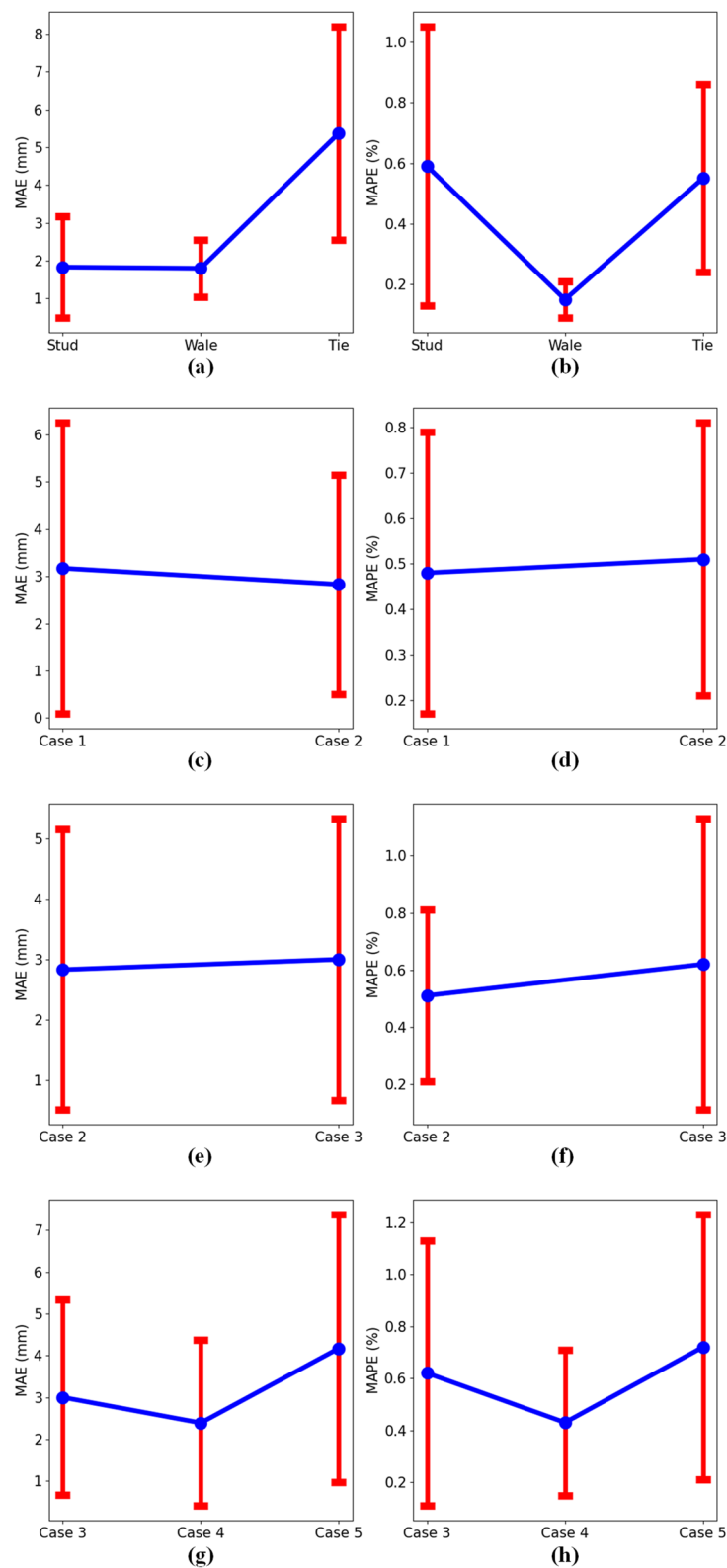


Figure 13. Comparison of the spacing measurement results: the stud, the wale, and the tie (a,b); Case 1 and Case 2 with different test objects (c,d); Case 2 and Case 3 with different numbers of scans (e,f); and Case 3, Case 4, and Case 5 with different distances of scans (g,h).

The first one is the orientation determination of the three principal axes in the transformed coordinate system. The orientation to fit formwork system members is a basis for

performing the automation of the spacing measurement, and it is used as a reference for the segmentation, identification, and recognition of formwork system members. Since the front surface of a stud is easier to be detected and has distinct shape features (i.e., length, width, and thickness are clearly different), it is used as the reference object for the transformation of the coordinate system. The coordinate system is transformed such that the orientation of the three principal axes can be determined following the shape of the stud front surface. In this way, the transformed coordinate system adapts well to the orientation of formwork system members, making segmentation, identification, and recognition easier.

The second one is the determination of the number of formwork system members in each category. Identifying the number of members in a formwork system is a prerequisite for the spacing measurement without human intervention. It is used to control the member detection, position identification, and spacing measurement processes, which can be stopped automatically when the corresponding number is reached. Studs and wales are installed along the second and first principal axes, respectively; therefore, the number of points for studs and wales varies regularly along the corresponding principal axes. Accordingly, the number of studs and wales can be determined using the multiple-peak detection algorithm applied along the corresponding principal axis. The number of these formwork system members is counted from the intersection between the baseline plotted across the average number of points and the distinct peak histograms. The size of ties is considerably smaller than that of braces; hence, the number of points for ties and braces is significantly different. Taking advantage of this, the number of ties and braces can be identified based on the variation of points with respect to a baseline. This baseline is determined by the average number of points over the total number of ties and braces.

The third one is the determination of the relative position of formwork system members in each category. To calculate the spacing between adjacent members, it is necessary to determine their relative positions. Therefore, the fact that a given category of formwork system members is installed along the corresponding principal axis (axes) is leveraged. Since studs are installed along the second principal axis, this implies that wales are installed along the first principal axis, braces are installed along the second principal axis, and ties are installed along the first and second principal axes. Their relative positions are established by comparing the mean values of the coordinates of points on the corresponding principal axis (axes). Consequently, the two adjacent members required for the spacing measurement can be identified by their sequentially assigned numbers, which are arranged in ascending order of mean values.

6. Conclusions and Outlook

This research proposed a framework for the spacing measurement of formwork system members with 3D point cloud data to enhance its automation. In summary, the proposed framework is divided into two parts. The first part is 3D point cloud data preprocessing, consisting of four steps: (1) remove surroundings, (2) remove outliers, (3) perform down-sampling, and (4) transform the coordinate system. The second part is 3D point cloud data processing and analysis, consisting of four steps: (1) segment remaining members, (2) identify the number of members, (3) recognize members, and (4) measure the spacing between members. The segmentation, identification, and recognition of formwork system members were fully automated without human intervention, although the removal of irrelevant surroundings around the formwork system being studied required some manual operations. A formwork system on an ongoing construction site was used to demonstrate the feasibility and effectiveness of the proposed framework. Five cases were considered with different test objects and scanning numbers and distances. When the 3D point cloud data approach was compared to the manual approach with a measuring tape and a laser distance meter for the five cases, the mean absolute error (MAE) and the mean absolute percentage error (MAPE) were 3.11 mm and 0.55%, respectively. The proposed framework was validated effectively, indicating that the 3D point cloud data approach is a promising solution and could potentially be an effective alternative to the manual approach.

There are some limitations to be further addressed in the proposed framework. When using 3D laser scanners to collect data, one needs to be mindful of highly reflective surfaces present in the scene that might introduce noise and false data in the process (i.e., ghost points introduced in the point cloud due to reflections). In these types of systems, it is common to have metal or highly reflective elements that would require a more thorough preprocessing stage. In addition, in spacious and big construction sites, scanning the surroundings of the formwork system is unavoidable. The points representing the surroundings are removed by applying the pass-through filter in the proposed framework. In this case, thresholds need to be determined manually by conforming to the 3D coordinates of the formwork system within the point cloud, which results in a prolonged step. In computer vision, machine learning techniques, including deep learning, have shown an excellent capability for object detection. It may be interesting to apply relevant techniques to detect the formwork system while excluding surroundings in the raw point cloud. Furthermore, some algorithms used in the proposed framework are required to set the corresponding computational parameters in advance. For example, the statistical outlier removal needs to set the number of neighbors and the threshold level based on the standard deviation of the average distances. However, the setting of such computational parameters relies largely on the scanning quality, and results may be different using the algorithm with the same computational parameters to process point clouds with different scanning quality. Therefore, an algorithm with the same computational parameters used for all point clouds without tuning is unreliable, especially on a construction site that easily suffers from surrounding factors (e.g., interference of different construction elements or activities). It will be valuable and challenging to develop more robust alternative algorithms. The above limitations could be investigated in future work.

Author Contributions: Conceptualization, K.W. and B.G.d.S.; methodology, K.W., S.A.P., E.M. and B.G.d.S.; formal analysis, K.W., S.A.P., E.M. and B.G.d.S.; investigation, K.W., S.A.P. and B.G.d.S.; data analysis, K.W., S.A.P., E.M. and B.G.d.S.; writing—original draft preparation, K.W. and B.G.d.S.; writing—review and editing, K.W., S.A.P., E.M. and B.G.d.S. All authors have read and agreed to the published version of the manuscript.

Funding: This research received no external funding.

Data Availability Statement: The data that support the findings of this study are available from the corresponding author upon reasonable request.

Acknowledgments: This work was partially supported by the NYUAD Center for Interacting Urban Networks (CITIES), funded by Tamkeen under the NYUAD Research Institute Award CG001, and the Sand Hazards and Opportunities for Resilience, Energy, and Sustainability (SHORES) Center, funded by Tamkeen under the NYUAD Research Institute Award CG013. Thanks to William Fulton and Mohamed Rasheed from the Campus Planning and Projects Office at NYUAD for their continuous support and for allowing access to ongoing projects on campus to test and implement our research.

Conflicts of Interest: The authors declare no conflicts of interest.

References

1. Hyun, C.; Jin, C.; Shen, Z.; Kim, H. Automated optimization of formwork design through spatial analysis in building information modeling. *Autom. Constr.* **2018**, *95*, 193–205. [\[CrossRef\]](#)
2. Li, W.; Lin, X.; Bao, D.W.; Xie, Y.M. A review of formwork systems for modern concrete construction. *Structures* **2022**, *38*, 52–63. [\[CrossRef\]](#)
3. Nunnally, S.W. *Construction Methods and Management*, 7th ed.; Pearson Prentice Hall: Hoboken, NJ, USA, 2007; ISBN 0-13-171685-9.
4. Wu, K.; Prieto, S.A.; García de Soto, B. Measuring the spacing of formwork system members using 3D point clouds. In Proceedings of the Creative Construction e-Conference 2022, Online, 9–11 July 2022; Budapest University of Technology and Economics: Budapest, Hungary, 2022; pp. 396–404. [\[CrossRef\]](#)
5. Ratay, R.T. Temporary structures in construction - USA practices. *Struct. Eng. Int.* **2004**, *14*, 292–295. [\[CrossRef\]](#)
6. Lee, B.; Choi, H.; Min, B.; Ryu, J.; Lee, D.-E. Development of formwork automation design software for improving construction productivity. *Autom. Constr.* **2021**, *126*, 103680. [\[CrossRef\]](#)
7. Nilimaa, J.; Gamil, Y.; Zhaka, V. Formwork engineering for sustainable concrete construction. *CivilEng* **2023**, *4*, 1098–1120. [\[CrossRef\]](#)

8. Tang, X.; Wang, M.; Wang, Q.; Guo, J.; Zhang, J. Benefits of terrestrial laser scanning for construction QA/QC: A time and cost analysis. *J. Manag. Eng.* **2022**, *38*, 05022001. [[CrossRef](#)]
9. Ma, Z.; Liu, S. A review of 3D reconstruction techniques in civil engineering and their applications. *Adv. Eng. Inform.* **2018**, *37*, 163–174. [[CrossRef](#)]
10. Mirzaei, K.; Arashpour, M.; Asadi, E.; Masoumi, H.; Bai, Y.; Behnood, A. 3D point cloud data processing with machine learning for construction and infrastructure applications: A comprehensive review. *Adv. Eng. Inform.* **2022**, *51*, 101501. [[CrossRef](#)]
11. Jiang, S.; Feng, X.; Zhang, B.; Shi, J. Semantic enrichment for BIM: Enabling technologies and applications. *Adv. Eng. Inform.* **2023**, *56*, 101961. [[CrossRef](#)]
12. Wang, Q.; Kim, M.-K. Applications of 3D point cloud data in the construction industry: A fifteen-year review from 2004 to 2018. *Adv. Eng. Inform.* **2019**, *39*, 306–319. [[CrossRef](#)]
13. Wang, Q.; Tan, Y.; Mei, Z. Computational methods of acquisition and processing of 3D point cloud data for construction applications. *Arch. Comput. Methods Eng.* **2020**, *27*, 479–499. [[CrossRef](#)]
14. Aryan, A.; Bosché, F.; Tang, P. Planning for terrestrial laser scanning in construction: A review. *Autom. Constr.* **2021**, *125*, 103551. [[CrossRef](#)]
15. Wu, C.; Yuan, Y.; Tang, Y.; Tian, B. Application of terrestrial laser scanning (TLS) in the architecture, engineering and construction (AEC) industry. *Sensors* **2022**, *22*, 265. [[CrossRef](#)] [[PubMed](#)]
16. “Definitions”, What Is ASPRS? Available online: <https://www.asprs.org/a/society/about.html> (accessed on 8 March 2024).
17. Mengiste, E.; Prieto, S.A.; García de Soto, B. Comparison of TLS and photogrammetric 3D data acquisition techniques: Considerations for developing countries. In Proceedings of the 39th International Symposium on Automation and Robotics in Construction, Bogotá, Colombia, 13–15 July 2022. [[CrossRef](#)]
18. Wang, Q.; Cheng, J.C.P.; Sohn, H. Automated estimation of reinforced precast concrete rebar positions using colored laser scan data. *Comput. Aided Civ. Infrastruct. Eng.* **2017**, *32*, 787–802. [[CrossRef](#)]
19. Zhao, W.; Jiang, Y.; Liu, Y.; Shu, J. Automated recognition and measurement based on three-dimensional point clouds to connect precast concrete components. *Autom. Constr.* **2022**, *133*, 104000. [[CrossRef](#)]
20. Kim, M.-K.; Wang, Q.; Park, J.-W.; Cheng, J.C.P.; Sohn, H.; Chang, C.-C. Automated dimensional quality assurance of full-scale precast concrete elements using laser scanning and BIM. *Autom. Constr.* **2016**, *72*, 102–114. [[CrossRef](#)]
21. Kim, M.-K.; Cheng, J.C.P.; Sohn, H.; Chang, C.-C. A framework for dimensional and surface quality assessment of precast concrete elements using BIM and 3D laser scanning. *Autom. Constr.* **2015**, *49*, 225–238. [[CrossRef](#)]
22. Kim, M.-K.; Sohn, H.; Chang, C.-C. Automated dimensional quality assessment of precast concrete panels using terrestrial laser scanning. *Autom. Constr.* **2014**, *45*, 163–177. [[CrossRef](#)]
23. Shu, J.; Li, W.; Zhang, C.; Gao, Y.; Xiang, Y.; Ma, L. Point cloud-based dimensional quality assessment of precast concrete components using deep learning. *J. Build. Eng.* **2023**, *70*, 106391. [[CrossRef](#)]
24. Yoon, S.; Wang, Q.; Sohn, H. Optimal placement of precast bridge deck slabs with respect to precast girders using 3D laser scanning. *Autom. Constr.* **2018**, *86*, 81–98. [[CrossRef](#)]
25. Wang, Q.; Kim, M.-K.; Cheng, J.C.P.; Sohn, H. Automated quality assessment of precast concrete elements with geometry irregularities using terrestrial laser scanning. *Autom. Constr.* **2016**, *68*, 170–182. [[CrossRef](#)]
26. Kim, M.-K.; Wang, Q.; Yoon, S.; Sohn, H. A mirror-aided laser scanning system for geometric quality inspection of side surfaces of precast concrete elements. *Measurement* **2019**, *141*, 420–428. [[CrossRef](#)]
27. Kim, M.-K.; Thedja, J.P.P.; Wang, Q. Automated dimensional quality assessment for formwork and rebar of reinforced concrete components using 3D point cloud data. *Autom. Constr.* **2020**, *112*, 103077. [[CrossRef](#)]
28. Kim, M.-K.; Thedja, J.P.P.; Chi, H.-L.; Lee, D.-E. Automated rebar diameter classification using point cloud data based machine learning. *Autom. Constr.* **2021**, *122*, 103476. [[CrossRef](#)]
29. Yuan, X.; Smith, A.; Sarlo, R.; Lippitt, C.D.; Moreu, F. Automatic evaluation of rebar spacing using LiDAR data. *Autom. Constr.* **2021**, *131*, 103890. [[CrossRef](#)]
30. Bosché, F. Automated recognition of 3D CAD model objects in laser scans and calculation of as-built dimensions for dimensional compliance control in construction. *Adv. Eng. Inform.* **2010**, *24*, 107–118. [[CrossRef](#)]
31. Liu, J.; Zhang, Q.; Wu, J.; Zhao, Y. Dimensional accuracy and structural performance assessment of spatial structure components using 3D laser scanning. *Autom. Constr.* **2018**, *96*, 324–336. [[CrossRef](#)]
32. Wang, Q. Automatic checks from 3D point cloud data for safety regulation compliance for scaffold work platforms. *Autom. Constr.* **2019**, *104*, 38–51. [[CrossRef](#)]
33. Zhao, L.; Mbachu, J.; Wang, B.; Liu, Z.; Zhang, H. Installation quality inspection for high formwork using terrestrial laser scanning technology. *Symmetry* **2022**, *14*, 377. [[CrossRef](#)]
34. CloudCompare—Open Source Project. Available online: <https://www.danielgm.net/cc/> (accessed on 8 March 2024).
35. Hodge, V.; Austin, J. A survey of outlier detection methodologies. *Artif. Intell. Rev.* **2004**, *22*, 85–126. [[CrossRef](#)]
36. Fischler, M.A.; Bolles, R.C. Random sample consensus: A paradigm for model fitting with applications to image analysis and automated cartography. *Commun. ACM* **1981**, *24*, 381–395. [[CrossRef](#)]
37. Wold, S.; Esbensen, K.; Geladi, P. Principal component analysis. *Chemom. Intell. Lab. Syst.* **1987**, *2*, 37–52. [[CrossRef](#)]
38. Ester, M.; Kriegel, H.-P.; Sander, J.; Xu, X. A density-based algorithm for discovering clusters in large spatial databases with noise. *KDD-96 Proc.* **1996**, *96*, 226–231.

39. Leica, "LEICA BLK360 Imaging Scanner 3D Reality Now". 2019. Available online: https://shop.leica-geosystems.com/sites/default/files/2019-04/blk360_spec_sheet_2_0.pdf (accessed on 8 March 2024).
40. Trimesh Library. Available online: <https://trimesh.org/> (accessed on 8 March 2024).
41. PyTorch3D · A Library for Deep Learning with 3D Data. Available online: <https://pytorch3d.org/> (accessed on 8 March 2024).
42. Open3D: A Modern Library for 3D Data Processing. Available online: <https://open3d.org/> (accessed on 8 March 2024).
43. OpenSfM. Available online: <https://opensfm.org/> (accessed on 8 March 2024).
44. "Point Cloud Library", Point Cloud Library. Available online: <https://pointcloudlibrary.github.io/> (accessed on 8 March 2024).
45. PDAL—Point Data Abstraction Library. Available online: <https://pdal.io/en/2.6.3/> (accessed on 8 March 2024).

Disclaimer/Publisher's Note: The statements, opinions and data contained in all publications are solely those of the individual author(s) and contributor(s) and not of MDPI and/or the editor(s). MDPI and/or the editor(s) disclaim responsibility for any injury to people or property resulting from any ideas, methods, instructions or products referred to in the content.